Date of submission:
July 8th, 2010

Title of journal:
Near Surface Geophysics

Title of paper:
Interpretation of microtremor 2D array data using Rayleigh and Love waves: the case study of Bevagna (central Italy)

Authors names and affiliations:
Puglia R.[1], Tokeshi K.[2,5], Picozzi M.[3], D'Alema E.[4], Parolai S.[3], Foti S.[2]

1. Istituto Nazionale di Geofisica e Vulcanologia, Sezione di Milano-Pavia, via Bassini 15, Milan, Italy
2. Politecnico di Torino, corso Duca degli Abruzzi 24, Torino, Italy
3. Helmholtz Centre Potsdam - German Research Centre For Geosciences (GFZ), Helmholtzstraße 7, 14467 Potsdam, Germany
4. Istituto Nazionale di Geofisica e Vulcanologia, Centro Nazionale Terremoti, strada Provinciale Cameranense snc, Passo Varano, Ancona, Italy
5. University of Western Sydney, Civionics Research Centre, Penrith campus, second avenue, Kingswood, NSW 2747, Australia

E-mail: ken.tokeshi@polito.it

Keywords:
Rayleigh waves, Love waves, surface-waves dispersion, ESAC, f-k spectra, genetic algorithm inversion, Monte Carlo inversion, passive microtremor measurements

Interpretation of microtremor 2D array data using Rayleigh and Love waves: the case study of Bevagna (central Italy)

Puglia R.[1], Tokeshi K.[2,5], Picozzi M.[3], D'Alema E.[4], Parolai S.[3], Foti S.[2]

1. Istituto Nazionale di Geofisica e Vulcanologia, Sezione di Milano-Pavia, via Bassini 15, Milan, Italy
2. Politecnico di Torino, corso Duca degli Abruzzi 24, Torino, Italy
3. Helmholtz Centre Potsdam - German Research Centre For Geosciences (GFZ), Helmholtzstraße 7, 14467 Potsdam, Germany
4. Istituto Nazionale di Geofisica e Vulcanologia, Centro Nazionale Terremoti, strada Provinciale Cameranense snc, Passo Varano, Ancona, Italy
5. University of Western Sydney, Civionics Research Centre, Penrith Campus, Second Avenue, Kingswood, NSW 2747, Australia

1. Abstract

In the last decades, geophysicists and seismologists have focused their attention on the inversion of empirical surface-waves' dispersion curves from microtremor measurements for estimating the S-waves velocity structure at a site. This procedure allows a fast and convenient investigation without strong active sources, which are difficult to deploy especially in urban areas.
In this study we report on a 2D seismic noise array experiment carried out at Bevagna (Central Italy) near the station BVG of the Italian Accelerometric Network (RAN). The site was investigated within the DPC-INGV S4 Project (2007-2009). The Rayleigh- and Love- waves dispersion characteristics were estimated using different methods. The inversion of the dispersion curves was then performed independently, obtaining two estimations for the S-waves velocity profiles. The results of cross-hole logging near the seismic station are used for a comparison.
The shear waves velocity profiles estimated by microtremor analyses range up to 150m depth. The two independent procedures provide consistent shear waves velocity profiles for the shallow part of the model (20-30 m in depth) in agreement with the results of the cross-hole logging. Some problems arise between 30 and 40 m in depth in the profile estimated by surface waves. In this range cross-hole logging evidences an inversion of S-waves velocity. Although the cross-hole logging stops at 40 m of depth, we are confident about the results provided by the Rayleigh-waves analysis below 40-50 m. This case study suggests that greater efforts should be devoted to exploit the potential of a coupled analysis of Rayleigh and Love waves from microtremor array measurements.

2. Introduction

Surface waves analysis provides efficient tools for the estimation of the shear waves velocity profile of a site at different scales (see Socco *et al*., 2010 and Foti et al., 2011, for an overview on this topic). In particular, the analysis of seismic noise recorded by 2D arrays offers the opportunity to characterize a site down to great depths (hundred meters to kilometres) avoiding the need of large and heavy active sources (Horike, 1985; Tokimatsu, 1997; Okada, 2003; Ohrnberger *et al*., 2004; Parolai *et al*., 2006). Often the analysis is based on the vertical components of microtremors, therefore focusing on studying the propagation of Rayleigh waves. However, since seismic noise recordings are typically collected using 3 component geophones, the horizontal components of ground motion can be used to infer information about Love waves propagation (Tokimatsu, 1997; Köhler *et al*., 2007; Fäh *et al*., 2008). Moreover, the 3 component recordings at each station of the array offer the opportunity to estimate the H/V spectral ratio (Nakamura, 1989; Lermo and Chavez-

Garcia, 1994). The latter provides information about the resonant frequency of a site, and can be used as an additional constraint in the inversion of surface waves dispersion curves (Parolai *et al*., 2005). Finally, the spatial variability of the horizontal-to-vertical spectral ratios of ambient vibrations (NHV) gives a qualitative estimate of the variability of ground properties in the study area. This allows the assumption of a 1D inversion scheme (i.e., assuming lateral homogeneity of the subsoil structure below the array) to be checked.

This work was carried out within the framework of Project S4 "The Italian strong motion database" (http://esse4.mi.ingv.it/), funded by the DPC-INGV (2007-09) agreement between the Italian Department of Civil Protection (DPC) and Istituto Nazionale di Geofisica e Vulcanologia (INGV).

In this study we present the results of a 2D array experiment performed at Bevagna (Central Italy). The microtremor 2D array experiment was performed close to the Italian Accelerometric Network (RAN) station BVG (Figure 1). The station is installed on a clayey formation (fluvial sediments in Figure 1b-c) which may modify the earthquake ground motion in the frequency band of engineering interest (e.g. residential buildings generally have their fundamental frequencies in the range 1-5 Hz). The shear waves velocity (V_S) is the most representative parameter for the subsoil seismic response; hence, its estimate is very important for both engineering and seismological purposes.

With regards to the seismicity of the Bevagna area, the database of the Italian strong motion records (Working Group ITACA, 2010) reports the second shock of the Umbria-Marche sequence (1997-09-26 09:40:25, M_W=6.0, epicentral distance: 22 km) as the earthquake characterized by the highest peak ground acceleration (78 cm/s^2) recorded at station BVG. The current Italian code *Norme tecniche per le costruzioni* (DM 14/01/2008) classifies the Bevagna area as medium-high hazard, in particular the peak ground acceleration with the 10% of probability of exceedance in 50 years – evaluated on the 50th percentiles – is equal to 0.200-0.225 g (on outcropping rock).

Seismic noise measurements in 2D array configuration were carried out by INGV-Milano in September 2007. Rayleigh- and Love- waves dispersion curves were estimated using two different methods. The inversion of the two dispersion curves was run independently in order to assess the effectiveness of the two approaches. For brevity, hereafter these two approaches are simply referred to as Rayleigh and Love analyses. In both analyses NHV spectral ratios were used to extend the low frequency limit that can be investigated considering the geometry of the array, allowing an increase in depth resolution.

The paper is organized as follows. After the description of the experimental dataset, with details on the acquisition and an assessment of spatial variability through NHV spectral ratios, we outline the procedures used for both Rayleigh- and Love- waves analyses. Finally, the results of the two independent inversions are compared to the shear waves velocity profile from an available cross-hole logging close to the station BVG (cf. Figure 1c) undertaken within the framework of the DPC-INGV S6 Project (http://esse6.mi.ingv.it/), which was provided to us after the completion of the Rayleigh- and Love- waves analyses.

3. Experimental dataset and estimation of the NHV curve

Seismic noise data were recorded for more than 3 hours using 15 Reftek 130 acquisition systems equipped with short-period Lennartz LE-3D/5s sensors and GPS timing. The sampling rate was fixed to 500 Hz, that is adequate for the investigated frequency range and the considered minimum inter-station distance of about 9 meters. For a given velocity, the lower is the minimum inter-station distance, the higher should be the sampling rate. In particular, the delay of a wave between two stations should be much higher than the chosen sampling rate. Note that the delay depends on wave velocity – which is an output of the inversion analysis – and therefore only plausible values for the shear waves velocities can be assumed when considering preliminary knowledge of the investigated site in order to fix the minimum interstation distance. The array geometry (Figure 2) was chosen in order to have a good coverage of both azimuths and of the inter-station distances between the minimum (about 10 m) and the maximum (about 150 m). These ranges allow the analysis of a range

of wavelengths that guarantee large depths to be investigated, but with still sufficient (i.e. from 5 to 10 m) shallow resolution (Okada, 2003).
Figure 3 shows the frequency-wavenumber response of the array (cf. Lacoss *et al*., 1969; Picozzi et al., 2010); this provides some insight into the expected limits in terms of the wavenumber k, of the valid array output. The response of the array shows a major aliasing peak at wavenumber 0.30 rad/m (cf. Figure 3). This peak does not reach the mid-height of the central peak, a value that was suggested by Wathelet (2005) as the threshold for the aliasing and resolution limits of the array response.
It is a common practice during surface wave investigation to first verify the reliability of the one-dimensional site structure assumption (Aki, 1957; Okada, 2003). For this reason, we estimated the NHV spectral ratio for all the stations of the array. In fact, the uniformity of NHV spectral ratios provides a first indication that significant lateral V_S variations do not affect the volume under the array. In this work, the NHV spectral ratios were calculated according to Equation (1):

$$\mathrm{NHV} = \frac{\sqrt{\mathrm{NS}^2 + \mathrm{WE}^2}}{\mathrm{UP}} \qquad (1)$$

where, as usual, NS, WE and UP represent the Fourier spectra for each component of the records (respectively the north-south, west-east and the vertical components). Before the spectra computation, an instrumental correction was applied to the recordings, together with a band-pass filter between 0.1 to 20 Hz. For each station, 50 windows of 200 seconds were baseline corrected (mean and linear trend), then transformed into Fourier spectra and smoothed. The spectral ratios – calculated by Eq. (1) – were considered log-normally distributed to estimate the average NHV curve of the station in hand. The adopted smoothing operator was the Konno and Ohmachi (1998) one with b=40.
Figure 2 shows the NHV ratio for each station. A predominant peak at a frequency of about 1.3 Hz appears at all stations (Figure 2). Overall, the assumption of a vertically heterogeneous 1D model in the study area is generally well satisfied. Slight differences are recognizable for stations BE01, BE09 and BE13 located on the boundary of the array, where their different behaviour could be associated with lateral variations and/or close noise sources.
The NHV curves (Figure 2) were averaged to obtain a representative curve for the site (Figure 4). Microtremors recorded at BE01, BE09 and BE13 stations were not considered when constructing the mean NHV. Although LE-3D/5s sensors can reproduce frequencies in the range 0.2-40 Hz, the minimum reliable frequency considered here is 0.5 Hz, since the trend of NHV ratios at lower frequencies clearly shows a drift which is likely to be due to installation problems (cf. recordings BE02, BE05, BE06, BE08, BE11, BE12 and BE15 in Figure 2). Forbriger (2006) showed for broad-band sensors that a rising drift from high to low frequencies could be due to a tilting of the instrument.

4. Rayleigh-waves dispersion curve analysis

The Rayleigh-waves dispersion curve was estimated by analyzing the vertical component of the recorded seismic noise. In particular, the Extended Spatial Auto Correlation (ESAC; Ohori *et al*., 2002; Okada, 2003) and the Frequency-Wavenumber (f-k; Lacoss *et al*., 1969; Capon, 1969) methods were adopted. To estimate the S-waves velocity profile, Rayleigh-waves dispersion and NHV ratio curves were used in a joint inversion scheme (Parolai *et al*. 2005).
The first step of the analysis consisted of a visual inspection of the recordings from all stations. For each of them, about 50 synchronized signal windows of 60 seconds were selected, avoiding time periods affected by local disturbance, visually identified from the velocity time series and from the single window Fourier spectra and spectral ratio. Selected windows were considered to calculate the experimental Rayleigh-waves dispersion curves using both f-k and ESAC techniques (Parolai *et al*.,

2006). The ESAC Rayleigh-waves dispersion curve is obtained by minimizing the root mean square (RMS) of the differences between experimental and theoretical Bessel functions (Figure 5). Values differing by more than two standard deviations from those estimated by the best fitting functions are automatically discarded (red circles in Figure 5) and the procedure is repeated iteratively. For this dataset, data are also discarded whenever the inter-station distance is 1.5 times longer than the relevant wavelength. This latter condition has been imposed after trial and error tests to avoid the lack of coherency for wavelengths much smaller than the inter-sensor distance in hand. The f-k methods were applied following the procedures proposed by Lacoss *et al*. (1969) and Capon (1969). Figure 6 shows the good agreement between the Rayleigh waves dispersion curves estimated with ESAC and f-k approaches (beam-forming method) in the frequency range 2.5-3.5 Hz. Below 2.5 Hz, the f-k analysis provides larger phase velocities. The disagreement at lower frequencies was discussed in previous studies (e.g., Parolai *et al*., 2007), thus below 2.5 Hz the ESAC method was considered more reliable than the f-k. Above 3.5 Hz, phase velocities retrieved by the f-k analysis are affected by spatial aliasing. Furthermore, problems arise with the ESAC method in estimating the phase velocity at around 3 Hz.
The f-k analysis allows checking on the noise source distribution; one of the basic assumptions for the application of the ESAC method is indeed that the seismic noise wavefield is nearly isotropic. The location of peaks in the f-k spectra is representative of both the seismic noise sources' locations in terms of azimuth and of the surface waves velocity. In particular, the phase velocity c_0 can be estimated for each frequency f_0 applying Equation (2):

$$c_0 = \frac{2\pi \cdot f_0}{\sqrt{k_{xo}^{\ 2} + k_{yo}^{\ 2}}}, \qquad (2)$$

where the values of k_{xo} and k_{yo} represent the location of a peak in the f-k spectra. We took advantage of the f-k analysis to better understand the reason for the anomalous gap in information previously observed in the ESAC curve at around 3 Hz. Figure 7 shows the f-k spectra at various frequencies calculated following the maximum likelihood method. In Figure 7a, contour plots at 2.5, 2.8 and 3.0 Hz indicate the presence of noise propagating from two different directions. In particular, they show that the highest energy is propagating from the north with a phase velocity of about 500 m/s. On the other hand, the noise source coming from south-west is characterized by a much lower velocity (about 300 m/s). The presence of such strong directional and non-isotropic seismic noise sources, violate the basic ESAC assumption dealing with the nature of the seismic noise wavefield, and may thus explain why the ESAC method failed at around 3 Hz.
In Figure 8 (as green circles) and in Table 1, the phase velocities corresponding to the peaks of the f-k contour plot (Figure 7) are reported and compared with the f-k dispersion curve provided by the beam-forming analysis. The peaks with high velocity of propagation that appear on contour plots of the f-k power density function between 2.5 and 3 Hz may be probably due to human activities, but a clear identification of the source was not possible. However, the presence of a nearby irrigation channel (reported in blue in Figure 7b) might explain this source of noise.
Considering the observed limitations in frequency of the two methods (ESAC and f-k), we decided to combine the ESAC dispersion curve in the 1.3÷2.5 Hz and 3.5÷5 Hz ranges with the f-k dispersion curve in the 2.5÷3.5 Hz range. The obtained dispersion curve was then used for the inversion (white squares in Figure 6).

4.1 Estimation of soil profiles using genetic algorithm

The non-linear inversions were run with the procedure proposed by Parolai *et al*. (2005), using a genetic algorithm (Yamanaka and Ishida, 1996) which does not rely upon an explicit starting model and allows the identification of a solution close to the global minimum. The forward modeling of

Rayleigh waves phase velocities and NHV curves was performed under the assumption of vertically heterogeneous 1D earth model using the modified Thomson-Haskell method proposed by Wang (1999) and following the suggestions of Tokimatsu *et al*. (1992) and Arai and Tokimatsu (2004). The modeling was not restricted to the fundamental mode, preserving the possibility that higher modes participate in simulating the observed dispersion and NHV curves.
Various inversions were performed to estimate the S-waves velocity profile constrained by only the dispersion curve (hereafter "dispersion inversion") and by both the dispersion and NHV ratio curves (hereafter "joint inversion"). In Figures 9 and 10, the results relevant to both dispersion and joint inversions are presented, with the number of layers overlying the half-space in the model fixed to 5 (Table 2). Through a genetic algorithm a search over 100 (dispersion inversion) and 200 (joint inversion) generations of a population of 50 models was carried out (Figure 9b and 10b). The inversion was repeated starting from 8 different seed numbers, i.e., from a different population of initial models. In this way it was possible to improve the exploration of the model parameters space.
During the inversion procedure the thickness and shear waves velocity of each layer could vary within the pre-defined ranges. By contrast, for each layer, density was assigned a priori, while the compression waves velocity (V_P) was calculated through equation (3), after defining the values of the shear waves velocity (V_S):

$$V_P = 1.1 \cdot V_S + 1290 \qquad (3)$$

where both V_S and V_P are expressed in m/s. This empirical relationship was proposed and validated for deep soil deposits by Kitsunezaki *et al*. (1990). Such a crude estimation can be used because of the limited influence on the dispersion curve by the P-waves velocity (Xia *et al*., 1999; Arai and Tokimatsu, 2004).
Models are selected on the basis of a cost function defined after Herrmann *et al*. (1999), by equation (4):

$$\text{cost} = [(1-p)N + pK] \cdot \left\{ \frac{1-p}{N} \left[\sum_{j=1}^{N} \left(\frac{c_O(f) - c(f)}{c_O(f)} \right)^2 \right] + \frac{p}{K} \left[\sum_{j=1}^{K} \left(\frac{NHV_O(f) - NHV(f)}{NHV_O(f)} \right)^2 \right] \right\} \qquad (4)$$

considering empirical and computed NHV and Rayleigh-waves dispersion curves. In equation 4, the subscript "o" indicates observed data, whereas N and K are the number of data points in the dispersion (c) and NHV curves, respectively. The relative influence of both data sets is controlled by the parameter p. If p=0, then the inversion is performed using only the apparent dispersion curve (dispersion inversion), while the inversion relies exclusively on the NHV for p=1. In this application, the weight p=0.05 was chosen for the joint inversion after trial and error tests looking for the best compromise in fitting both curves.
In Figures 9a (dispersion inversion) and 10a (joint inversion) tested models are shown in different colors according to their cost value: the more reliable model (minimum cost) is in white, the models lying inside the 10% range of the minimum cost are in black, and the other tested models are shown in grey. The agreement between experimental and theoretical Rayleigh waves dispersion curves (gray and open circles in Figures 9c and 10c) is good and, considering the wavelengths related to the dispersion curve frequency range, the V_S profile between about 10 and 50 meters is very well constrained (cf. agreement between simulated and observed dispersion curve between 2.5 and 5Hz). At greater depths, until about 140 meters, which corresponds to the lower frequency (1.3 Hz) at which the dispersion curve has been estimated, the agreement between the two curves is not completely satisfactory (cf. Figures 9c and 10c). For this reason, below 50 m depth the inversion

based on dispersion curve only (Figure 9a) proposed a high number of plausible models, i.e., models lying inside the minimum cost plus the 10% range (black lines). On the contrary, the inversion of the NHV curve (Figure 10d) allows us to restrict the number of model that can equally reasonably explain the different data-sets. In particular, the joint inversion scheme provides, after the very well constrained shear waves velocity contrast at a depth of 20m (from about 130 to 320 m/s), a V_S in the clayey formation that seems to gradually increase until 450 m/s at 150m (cf. Figure 10a).

5. Love waves dispersion curve analysis

In order to estimate the Love-waves dispersion curve, we implemented the procedure proposed by Tokimatsu (1997) under the assumption that some noise segments of the transversal horizontal component of microtremors mainly consist of Love waves. An undersampling of microtremor records to 100 Hz was applied to simplify data processing. The method requires a preliminary analysis of several segments of the vertical component of ground motion with the aim of detecting a possible azimuthal alignment (similar predominant directional angles) of seismic sources for a certain frequency band. The directional angles were estimated using the f-k spectral method (beam forming) with software developed by the Natural Research Institute for Earth Science and Disaster Prevention of Japan - NIED (http://www.bosai.go.jp/). In the next step, the horizontal components are rotated with respect to the seismic sources, and the f-k analysis is performed on the transversal component of ground motion to retrieve Love waves velocities.

Twelve noise segments of 80 s for stations BE02 to BE12 (except BE09) were considered simultaneously. The decomposed transversal and radial components were obtained by rotating 20° the horizontal components. The angle of rotation was chosen after searching for similar predominant source directionalities in the f-k spectra of the vertical, transversal and radial components. Figure 11 shows the predominant directional angles of the 3 components (vertical, transversal and radial components) obtained from a single frame of 80 s. The results are consistent in the frequency range 1.4-2.7 Hz with a predominant angle of 20°. Two examples of transversal f-k spectra obtained for 2 and 2.7 Hz are shown in Figure 12, where the predominant directional angles are around 20°. Note that similar predominant source directions were obtained in the f-k spectra presented in the previous section (Fig. 7). As mentioned before, these seismic sources could be originated from the "Statale dei Monti Martani" street and/or an irrigation channel (Fig. 7b).

The experimental Love-waves dispersion curve is plotted in Figure 13 together with the Rayleigh waves dispersion curve obtained using the vertical components for the same dataset. Note that the lowest retrieved frequency is 1.3 Hz, which is the same value as the predominant NHV spectral ratio frequency in Fig. 4. The use of Love waves allows the investigation of a larger frequency range (1.3 – 3.2 Hz) compared to Rayleigh-waves (1.5 – 2.1 Hz). It is important to note that the Rayleigh-waves dispersion curve of Figure 13 was obtained using the f-k spectral method (beam forming), hence it is an independent estimate with respect to that of Section 4.

5.1 Estimation of soil profiles using random search

For the inversion of the Love-waves dispersion curve (assumed to be the fundamental mode), we adopted a ground model consisting of 4 horizontal layers overlying an half-space (Table 3). A random search (Monte Carlo inversion) on three parameters (S-waves velocity, thickness and Poisson's ratio) for each layer was employed. The first two parameters, the S-waves velocity and the thickness, have a strong influence on the Love-waves phase velocities. Another parameter that affects the dispersion curves is the density (Xia *et al*., 1999), which is estimated with an empirical correlation with the P-waves velocity (Gardner *et al*., 1974). In turn, the latter is correlated with the Poisson's ratio and the S-waves velocity (Tokeshi *et al*., 2008).

One million trials were performed during the random search. In order to improve the efficiency of the algorithm, the value of the SH-wave resonance frequency of each model was calculated and compared with the predominant NHV spectral frequency obtained from microtremors (1.3 Hz in

Fig. 4). The random models that have a SH-wave resonance frequency higher than the resonance frequency obtained through NHV, shows a Love-wave theoretical fundamental dispersion mode that will not fit the experimental Love-wave dispersion curve in the low frequency range (close to 1.3 Hz). Therefore, only the subsoil models having resonance frequencies lower than 1.3 Hz have been considered for the next step. The theoretical Love-waves fundamental mode for each subsoil model was then compared with the observed one. We determined how many points of the theoretical phase velocity pass within the relative error of 10% of the observed phase velocity (black hyphen in Figure 13). The acceptable subsoil models are ordered according to the number of points that satisfied the previous condition and the least-square-misfit criterion.
Figure 13 shows the comparison between the observed and the theoretical dispersion curves for the Love-waves fundamental mode of the 7 best solutions. These models have also been used to calculate the associated theoretical dispersion curve for the Rayleigh-waves fundamental mode. Although the inversion was performed only using the Love-waves dispersion curve as input, the agreement of observed and theoretical fundamental modes is quite good for both the Love- and Rayleigh- waves.
The lowest retrieved frequency (1.3 Hz) is associated to a phase velocity of 740 m/s (Figure 13). This value can be considered a threshold which separates the reliable and the less reliable portion of the estimated Vs profiles. The layers with Vs values higher than the available highest experimental phase velocity (red dotted lines in Fig. 14) have a low reliability.

6. Comparison of Rayleigh- and Love- waves analyses with cross-hole test

Independent Rayleigh- and Love- waves inversions provide consistent shear-waves velocity profiles for the shallow part of the model (Figure 14). Moreover the two inversions provide an estimate of the thickness (20 meters) and shear-waves velocity (120-150 m/s) of the first layer (clayey formation) in agreement with the results of a nearby cross-hole (CH) test (Figure 14).
Below 20 m, the Rayleigh waves inversion identifies a layer with an estimated V_S of 320 m/s. We believe that this shear-waves velocity represents an average value of the V_S at depths between 20 to 100 m. In fact, the CH test finds higher values of V_S especially between 20 to 30 m, but the Rayleigh waves dispersion curve is very well reconstructed for frequencies higher than 2.5 Hz (cf. Figure 10c), that is for depth lower than 50 m. Furthermore, although the Rayleigh-waves analysis takes into account higher modes, it was not able to reproduce the velocity inversion seen in the CH test. Probably, the problem for which the velocity inversion could not be resolved in the Rayleigh-wave analysis is the strong directional noise around 3Hz. In fact the reconstruction of the dispersion curve in this range of frequencies was very complex and probably not perfect (cf. Figure 6). This range of frequencies corresponds to 20÷40 m of depth, exactly where the cross-hole logging evidences the velocity inversion.
On the other hand, the estimated soil profiles for Love-waves analysis are consistent with the CH results between 20 and 35 m of depth, but suggest an overestimate of the CH measurements below 35 m. This is likely to be due to the adopted model parameterization; indeed the limited number of layers didn't allow the velocity inversion to be identified. Furthermore, in the Rayleigh analysis, higher modes are also taken into account, while the Love inversion is performed on the fundamental mode and this probably limits the detection of a velocity inversion. At depths greater than 60 m the subsoil profiles obtained by the Love waves analysis are not considered reliable because the experimental data are not sufficient to constraint adequately the inversion (as shown by the red dashed lines in Fig. 14).

7. Conclusion

In the present work Rayleigh- and Love- waves analyses have been carried out in parallel and an a-posteriori comparison of the results with a cross-hole measurement is reported. The two approaches exploit the information that can be extracted from microtremor measurements using 2D arrays of 3 components sensors. In the reported case history, the fundamental mode inversion of the Love

dispersion curve seems to furnish a better estimate of the S-wave velocities in the shallow part of the investigated soil down to 30 m of depth, while the Rayleigh-waves inversion analysis, constrained by both the dispersion curve and the complete reproduction of the NHV spectral ratio, can reach higher depth, down to 150 m. Rayleigh-wave analysis failed in detecting the velocity inversion seen in the CH test at a depth of 30 m, probably because of the presence of strong directional seismic noise sources at frequencies around 3 Hz. Unfortunately, the CH test stops at 40 m and it was not possible to compare the results obtained with the Rayleigh-waves inversions analysis at greater depth. Nevertheless, we are confident about the results provided by the Rayleigh-waves analysis below 40-50 m because of the Rayleigh-waves dispersion curve seems adequately reconstructed in the range 1.4-2.5 Hz.

Totally independent analyses have been performed in this study. A combined inversion of Rayleigh and Love waves dispersion with NHV spectral ratios could improve the estimation of the S-waves velocity profile. This is particularly true if higher modes are taken into account, because Love-waves are expected to be more sensitive with respect to velocity inversions. In addition, this case history showed that in a site which presents a complex geophysical-geotechnical background, such as a probable shear waves velocity inversion, at least the first 20m of the subsoil profile can be characterized even without any a-priori information. Moreover, the averaged S-waves velocity structure can be retrieved from the surface waves analyses, reducing the costs with respect to invasive measurements such as cross-hole or a down-hole tests.

Acknowledgments

This work is part of the INGV-DPC S4 Research Project "Italian Strong Motion Data Base", promoted by the Istituto Nazionale di Geofisica e Vulcanologia (INGV) and funded by the Dipartimento della Protezione Civile (DPC) of the Italian Government (Agreement INGV-DPC 2007-2009). The authors wish to thank the DPC and the project team coordinators, Dr. Francesca Pacor and Prof. Roberto Paolucci, for their valuable scientific and administrative support. The INGV-Mi team (composed of Dr. Dino Bindi, Ezio D'Alema, Sara Lovati and Dr. Marco Massa) who previously executed the in situ microtremor measurements is also warmly acknowledged. Likewise, thanks to the Regione Piemonte for financing Ken Tokeshi's grant.

References

Aki, K., 1957. Space and time spectra of stationary stochastic waves, with special reference to microtremors. Bull. Earthq. Res. Inst., 35, 415-456.

Arai H. and Tokimatsu K. 2004. S-wave velocity profiling by inversion of microtremor H/V spectrum. Bull. Seism. Soc. Am., 94, 53–63.

Capon, J., 1969. High-resolution frequency-wavenumber spectrum analysis, Proc. IEEE, 57, 8, 1408-1418.

Fäh D., Stamm G. and Havenith H.-B. 2008. Analysis of three-component ambient vibration array measurements. Geophys J Int, 172:199–213, doi:10.1111/j.1365-246.X.2007.03625.x

Forbriger T. 2006. Low-frequency limit for H/V studies due to tilt. Extended Abstract, Sitzung der Arbeitsgruppe Seismologie des FKPE, Haidhof, Germany.

Foti S., Parolai S., Albarello D., Picozzi M. (2011) "Application of Surface-wave methods for seismic site characterization", Survey in Geophysics, Springer, in press, DOI: 10.1007/s10712-011-9134-2

Gardner G. H. F., Gardner L. W. and Gregory A. R. 1974. Formation velocity and density; the diagnostic basics for stratigraphic traps. Geophysics, 39, 770-780.

Herrmann R.B., Ammon C.J., Julia J. and Mokhtar T. 1999. Joint inversion of receiver functions and surface-wave dispersion for crustal structure. Proc. 21st Seismic Research Symposium Technologies for monitoring the comprehensive Nuclear test Ban treaty, September 21-24, 1999, Las Vegas, Nevada, USA, published by Los Alamos National Laboratory, LA-UR-99-4700.

Horike M. 1985. Inversion of phase velocity of long period Microtremors to the S-wave velocity structure down to the basement in urbanized areas. J. Phys. Earth 33, 59–96.
Kitsunezaki C., Goto N., Kobayashi Y., Ikawa T., Horike M., Saito T., Kurota T., Yamane K. and Okozumi K. 1990. Estimation of P- and S-wave velocities in deep soil deposits for evaluating ground vibrations in earthquake. J.JSNDS, 9, 1-17.
Köhler A., Ohrnberger M., Scherbaum F., Wathelet M., Cornou C. 2007. Assessing the reliability of the modified three-component spatial autocorrelation technique. Geophys. J. Int., Vol. 168, 779-796.
Konno K. and Ohmachi T. 1998. Ground-Motion Characteristics Estimated from Spectral Ratio between Horizontal and Vertical Components of Microtremor. Bull. Seism. Soc. Am., 88, 228-241.
Lacoss R.T., Kelly E.J. and Toksöz M.N. 1969. Estimation of seismic noise structure using arrays. Geophysics, 34, 21-38.
Lermo J., and Chavez-Garcia F. J. 1994. Are microtremors useful insite response evaluation ?. Bull. Seism. Soc. Am. 84, 1350–1364.
Nakamura Y. 1989. A method for dynamic characteristics estimation of subsurface using microtremor on the ground surface. QR RTRI 30, 25-33.
Ohori M., Nobata A. and Wakamatsu K. 2002. A comparison of ESAC and FK methods of estimating phase velocity using arbitrarily shaped microtremor analysis. Bull. Seism. Soc. Am., 92, 2323-2332.
Ohrnberger M., Scherbaum F., Kruger F., Pelzing R. and Reamer S. K. 2004. How good are shear-wave velocity models obtained from inversion of ambient vibrations in the lower Rhine embayment (N.W. Germany)? Boll. Geofis. Teor. Appl. 45, 215–232.
Okada H. 2003. The Microtremor Survey Method, Geophysical Monograph series 12, M. W. Asten (Editor), Society of Exploration Geophysicists, Tulsa, Oklahoma.
Parolai S., Picozzi M., Richwalski S.M. and Milkereit C. 2005. Joint inversion of phase velocity dispersion and H/V ratio curves from seismic noise recordings using a genetic algorithm, considering higher modes. Geoph. Res. Lett., 32, doi: 10.1029/2004GL021115.
Parolai S., Richwalski S.M., Milkereit C. and Fäh D. 2006. S-wave velocity profile for earthquake engineering purposes for the Cologne area (Germany). Bull. Earthq. Eng., 65–94, doi:10.1007/s10518-005-5758-2.
Parolai S., Mucciarelli M., Gallipoli M.R., Richwalski S.M. and Strollo A. 2007. Comparison of Empirical and Numerical Site Responses at the Tito Test Site, Southern Italy, Bull. Seism. Soc. Am., 97, 1413-1431.
Picozzi, M., Parolai, S., and Bindi, D. (2010). De-blurring of frequency-wavenumber images from small-size seismic arrays. Geophysical Journal International,181,1,357-368. DOI: 10.1111/j.1365-246X.2009.04471.x
Socco, L.V., Foti S. and Boiero D. 2010. Surface wave analysis for building near surface velocity models: established approaches and new perspectives. Geophysics 75(5), A83-A102
Tokeshi K., Karkee M. and Cuadra C. 2008. Estimation of Vs profile using its natural frequency and Rayleigh-wave dispersion characteristics. Adv. Geosci., 14, 75-77. www.adv-geosci.net/14/75/2008/.
Tokimatsu K., Tamura S. and Kojima H. 1992. Effects of multiple modes on Rayleigh wave dispersion characteristics. Journal of Geotechnical Engineering 118, 1529–1543.
Tokimatsu, K. 1997. Geotechnical Site Characterization using Surface Waves. Proceedings of the 1st International Conference on Earthquake Geotechnical Engineering, 1333–1368.
Wang R. 1999. A simple orthonormalization method for stable and efficient computation of Green's functions. Bulletin of the Seismological Society of America 89, 733–741.
Wathelet M. 2005. Array recordings of ambient vibrations: surface-wave inversion. Ph.D. Thesis, Université de Liège, Faculté des Sciences Appliquées.

Working Group ITACA, 2010. Data Base of the Italian strong motion records. http://itaca.mi.ingv.it/ItacaNet/ . Accessed on February 2011.
Xia J., Miller R. D. and Park C. B. 1999. Estimation of near-surface shear-wave velocity by inversion of Rayleigh waves. Geophysics, 64, 691-700.
Yamanaka H. and Ishida H. 1996. Application of Generic algorithms to an inversion of surface-wave dispersion data. Bull. Seism. Soc. Am. 86, 436-444.

LIST OF FIGURES

Figure 13 - Comparison of observed Love- and Rayleigh-wave dispersion curves obtained by f-k spectral method (beam forming) with the theoretical Love- and Rayleigh-wave fundamental modes of the 7 best estimated soil profiles.

Figure 14 - Comparison between the cross-hole results and the VS soil profiles based on observed Rayleigh and Love dispersion curves. The unreliable portion of the VS profiles provided by the Love wave analysis is depicted as red dots.

***

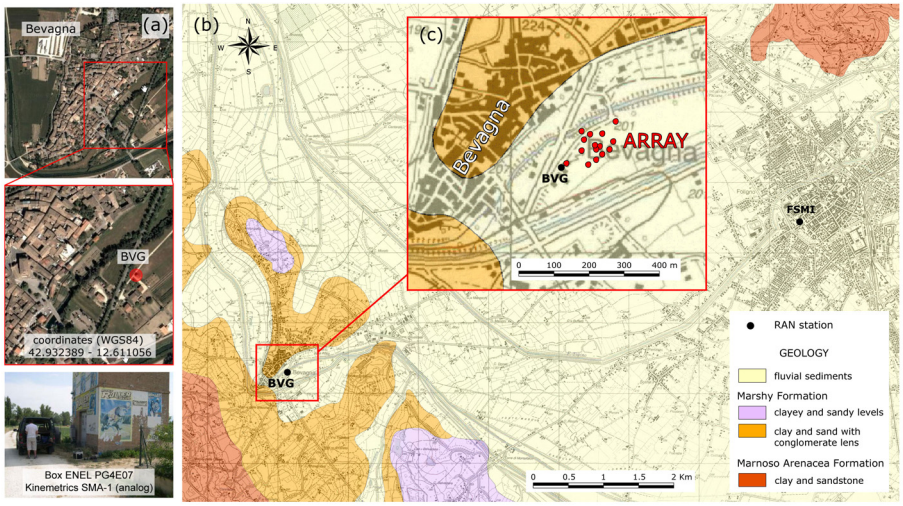

Figure 1 - (a) Location of the Italian accelerometric network station BVG. (b) Geological setting of the study area (from the geological sheet of Italy n. 131 at scale 100.000, ISPRA). (c) Relative position between the BVG station and the array measurements.

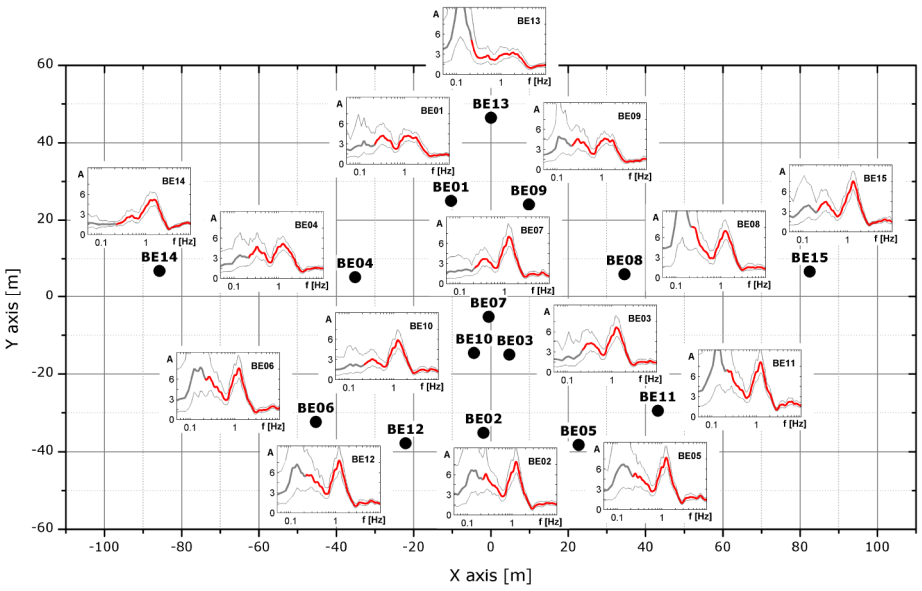

Figure 2 - Geometry of the array and NHV spectral ratios of the stations.

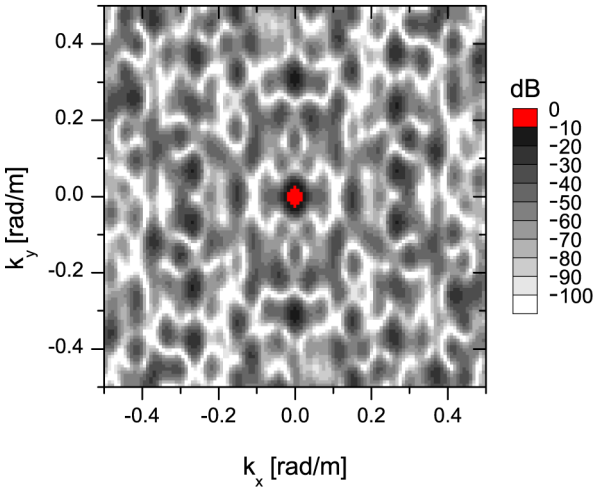

Figure 3 - f-k array response in dB.

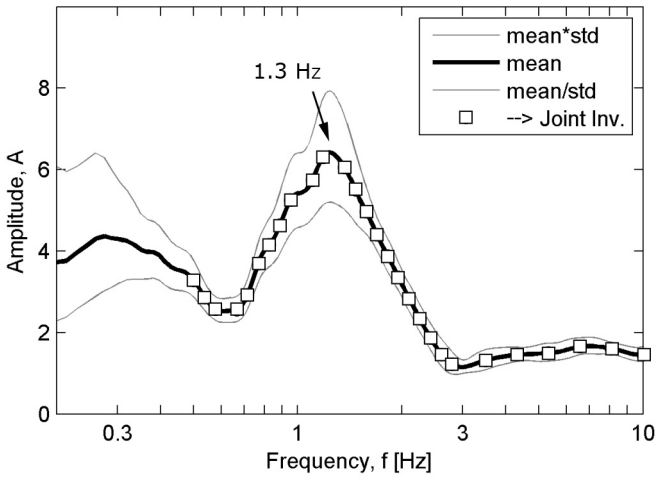

Figure 4 - NHV spectral ratio representative for the array. In the legend “std” stands for one standard deviation calculated considering a log-normally distribution of the NHV amplitudes. The white squares are used to constrain the Rayleigh-waves inversion.

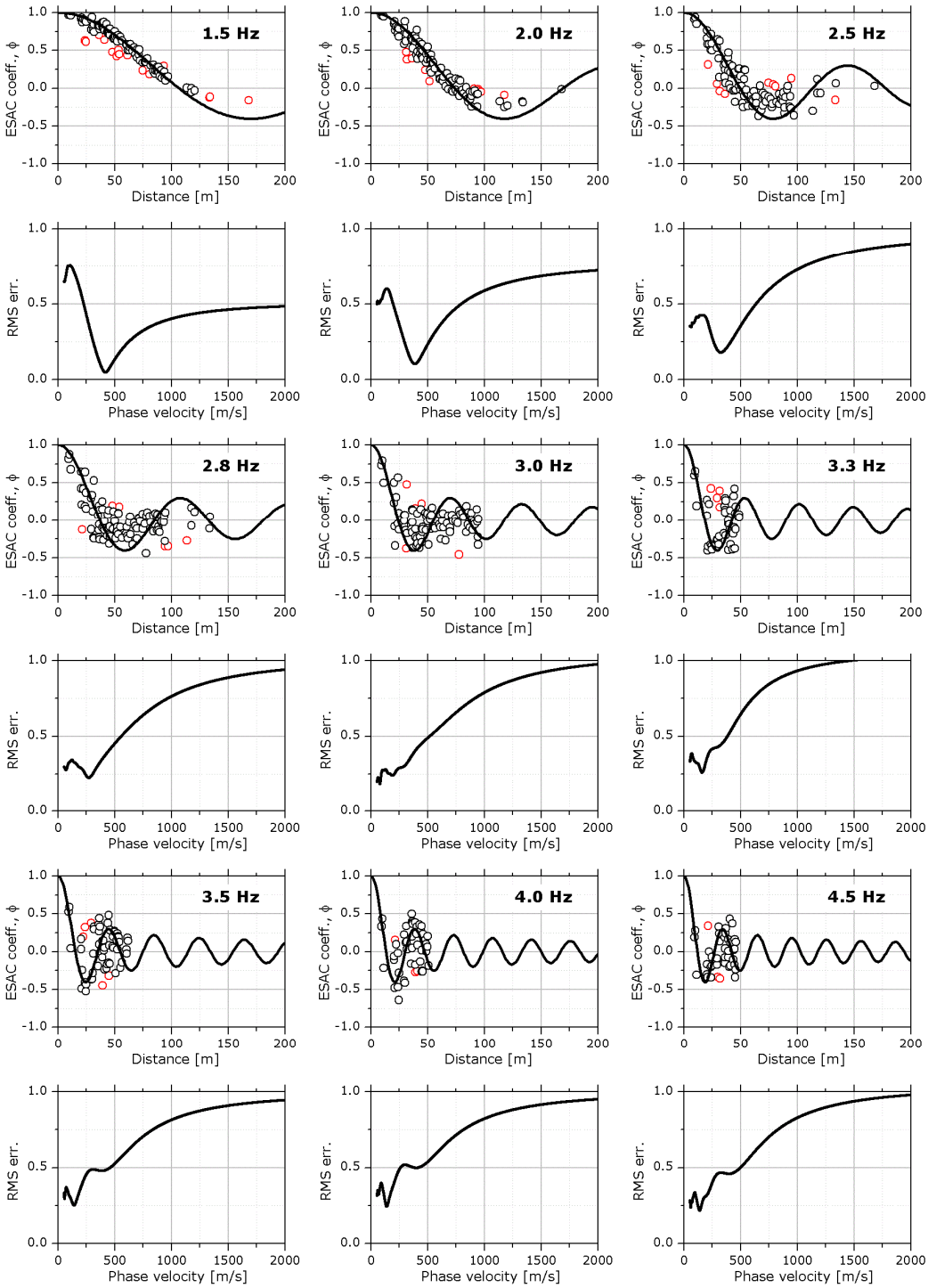

Figure 5 - Experimental space-correlation function values versus distance (circles) for different frequencies. The red circles indicate values that were discarded. The black lines depict the estimated space-correlation function values for the phase velocity that furnishes the best fit to the data. The bottom panels show the relevant root-mean square errors (RMS) versus phase velocity tested.

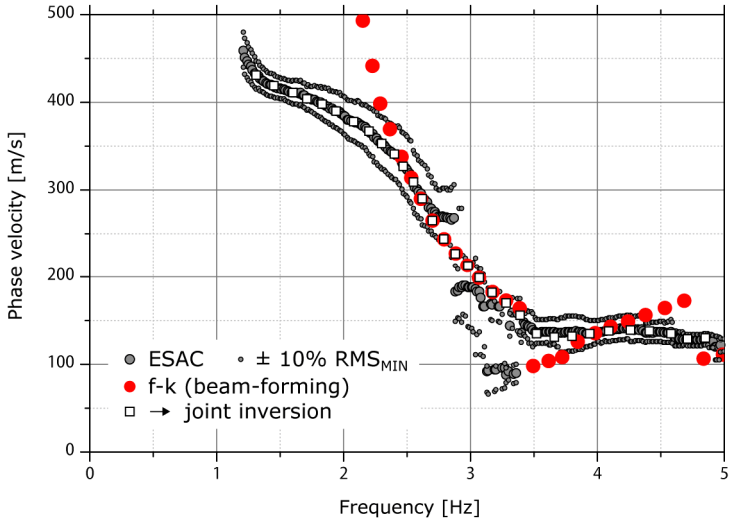

Figure 6 - Comparison of experimental phase velocities estimated by ESAC and f-k methods. Together with the ESAC dispersion curve, the 10% of the minimum root mean square (RMS) of the differences between experimental and theoretical Bessel function (cf. Figure 5 – bottom panels) are shown as little grey circles. The white squares represent the values used for the joint inversion.

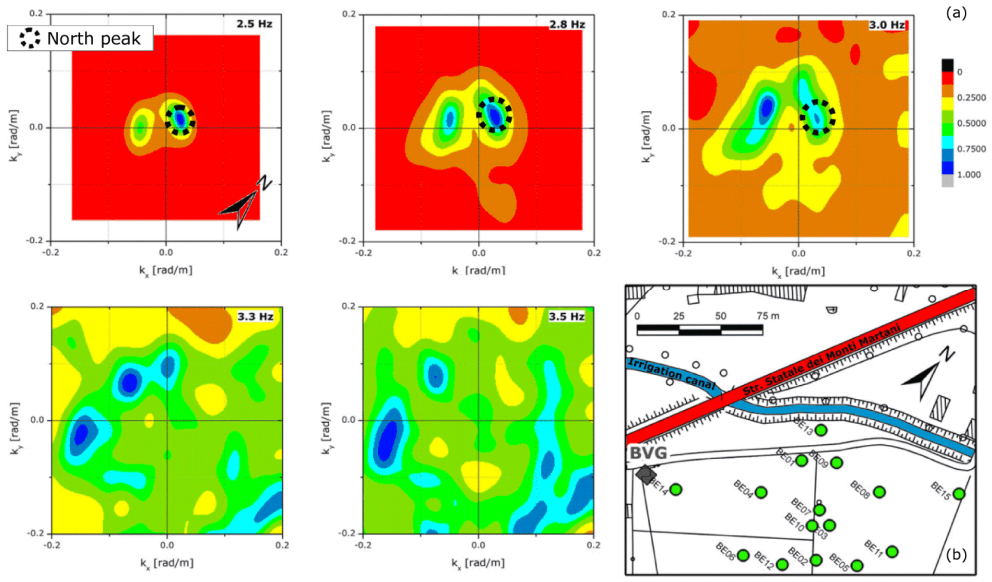

Figure 7 - (a) f-k power density function (maximum likelihood method) at different frequencies. (b) Map of the array measurement. Note the position of the "Statale dei Monti Martani" street and of an irrigation channel respect to the array.

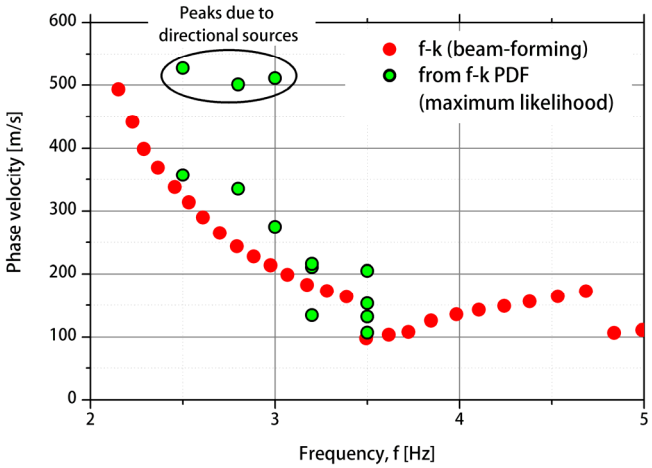

Figure 8 - Observed Rayleigh-wave dispersion curves estimated by two f-k methods (beam-forming and maximum likelihood). Green circles represent the phase velocities directly obtained through Equation 2 from peaks of maximum likelihood method power density functions (cf. Figure 7).

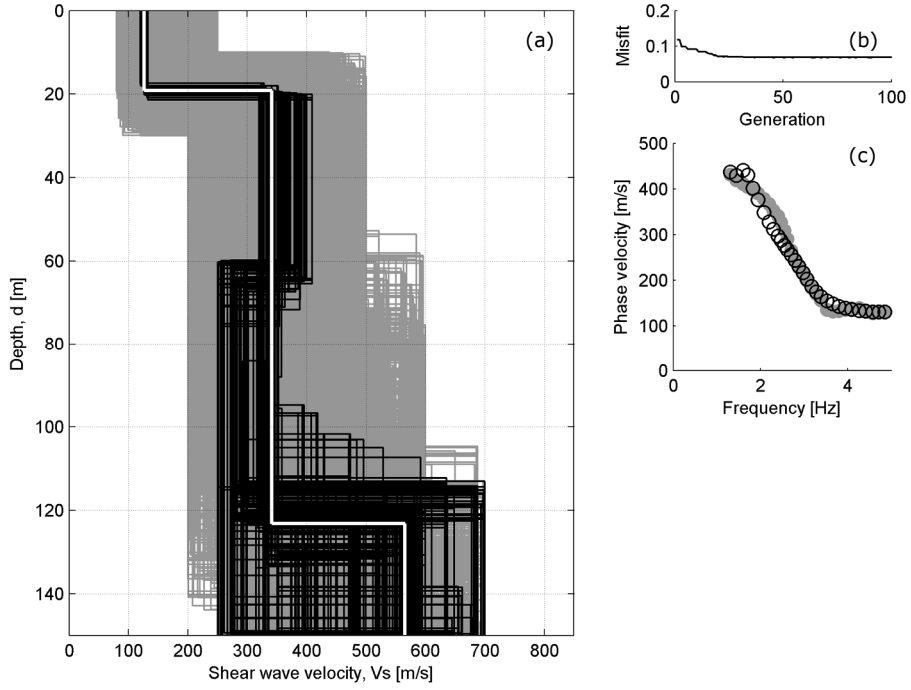

Figure 9 - (a) Shear wave velocity models at the BVG station constraining inversion with the only dispersion curve: tested models (grey lines), the minimum cost model (white line), and models lying inside the minimum cost + 10% range (black lines). (b) The generation values versus misfit. (c) The fitting to the dispersion of experimental data (grey circles) and empirical values relative to the minimum cost model (white circles).

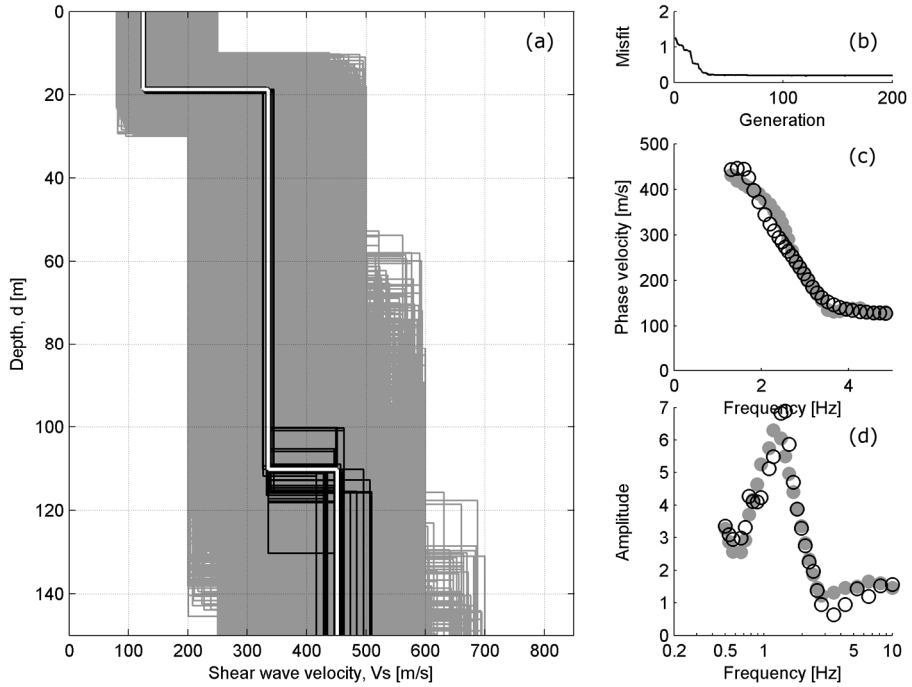

Figure 10 - (a) Shear wave velocity models at the BVG station using a joint inversion scheme: tested models (grey lines), the minimum cost model (white line), and models lying inside the minimum cost + 10% range (black lines). (b) The generation values versus misfit. (c) The fitting to the dispersion and (d) to the NHV ratio curves in terms of experimental data (grey circles) and empirical values relative to the minimum cost model (white circles).

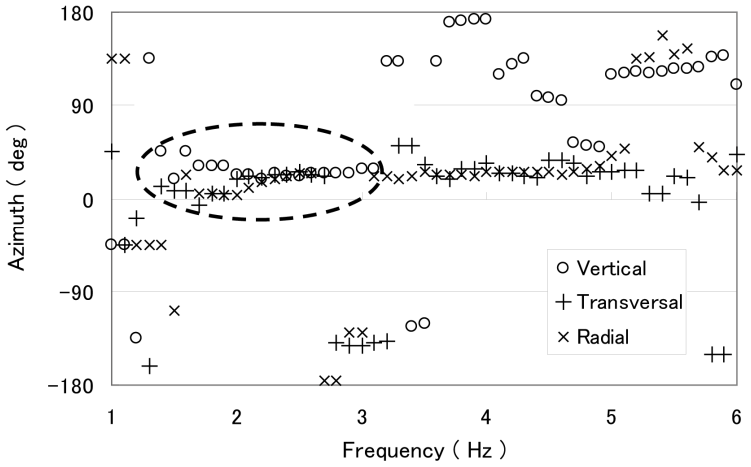

Figure 11 - Predominant directional angle of sources versus frequency obtained from vertical, transversal and radial f-k spectral analysis (80 s frame).

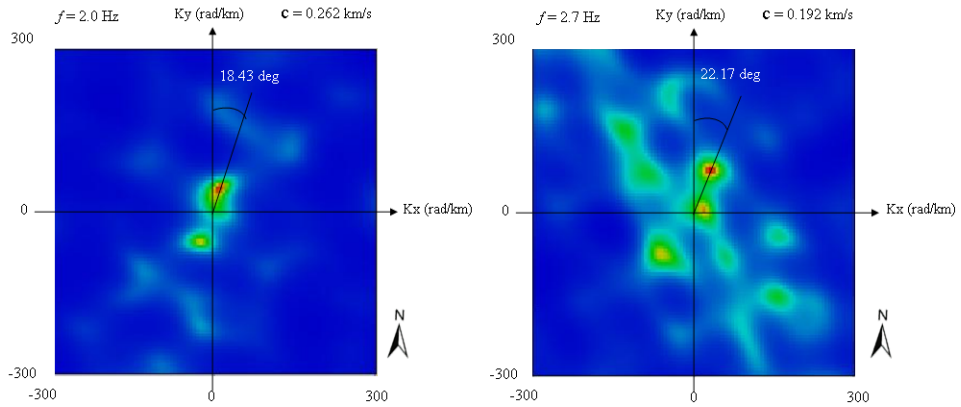

Figure 12 - f-k spectra obtained from transversal components of microtremor records.

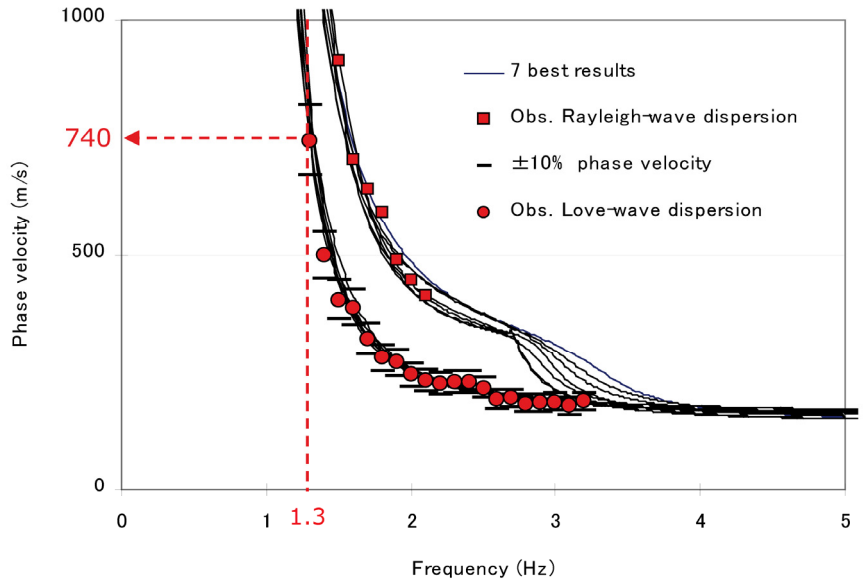

Figure 13 - Comparison of observed Love- and Rayleigh-wave dispersion curves obtained by f-k spectral method (beam forming) with the theoretical Love- and Rayleigh-wave fundamental modes of the 7 best estimated soil profiles.

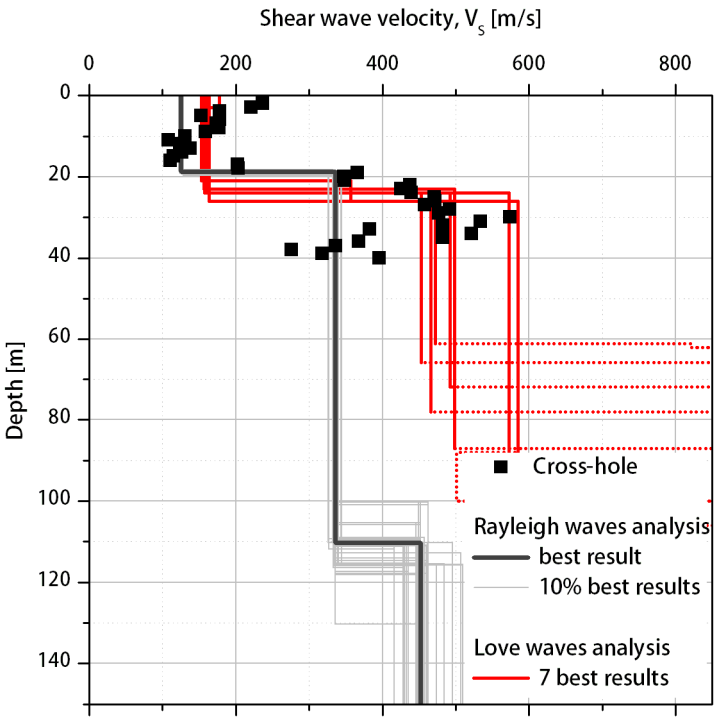

Figure 14 - Comparison between the cross-hole results and the V_S soil profiles based on observed Rayleigh and Love dispersion curves. The unreliable portion of the V_S profiles provided by the Love wave analysis is depicted as red dots.

LIST OF TABLES

***

Table 1 - Phase velocities directly obtained from f-k power density functions peaks through Equation 2.

f_0 [Hz]	k_{x0} [rad/m]	k_{y0} [rad/m]	c_0 [m/s]
2.5	*0.0247*	*0.0166*	*527*
	-0.0439	0.0008	357
2.8	*0.0294*	*0.0193*	*501*
	-0.0499	0.0161	335
3.0	*0.0314*	*0.0193*	*511*
	-0.0541	0.0422	275
3.2	0.0001	0.0954	211
	-0.0656	0.0663	216
	-0.1480	-0.0214	134
3.5	-0.0739	0.0777	205
	-0.1605	-0.0422	132
	0.0835	-0.1873	107
	0.1200	-0.0798	153

Table 2 - Parameters ranges used in the joint inversion of the Rayleigh-wave analysis.

	Shear wave velocity, V_S [m/s]		Thickness, h [m]		Density, ρ [ton/m^3]
Layer	MIN	MAX	MIN	MAX	
#1	80	250	10	30	1.9
#2	200	500	40	120	1.9
#3	250	600	50	160	2.1
#4	300	700	60	220	2.2
#5	400	800	150	700	2.2
Half-space	1000	3000	Infinite		2.3

Table 3 - Ranges used in parameters for random inverse analysis of the Love-wave dispersion curve.

	Poisson's ratio, ν		Shear wave velocity, V_S [m/s]		Thickness, h [m]	
Layer	MIN	MAX	MIN	MAX	MIN	MAX
#1	0.25	0.49	100	400	1	30
#2				700		100
#3				1000		100
#4				1500		100
Half-space	$V_P = 3800$ $V_S = 2500$				Infinite	